Stable Spectral Mesh Filtering

Artiom Kovnatsky[1], Michael M. Bronstein[1], and Alexander M. Bronstein[2]

[1] Institute of Computational Science, Faculty of Informatics,
Università della Svizzera Italiana, Lugano, Switzerland
{artiom.kovnatsky,michael.bronstein}@usi.ch
[2] School of Electrical Engineering, Tel Aviv University, Israel
bron@eng.tau.ac.il

Abstract. The rapid development of 3D acquisition technology has brought with itself the need to perform standard signal processing operations such as filters on 3D data. It has been shown that the eigenfunctions of the Laplace-Beltrami operator (manifold harmonics) of a surface play the role of the Fourier basis in the Euclidean space; it is thus possible to formulate signal analysis and synthesis in the manifold harmonics basis. In particular, geometry filtering can be carried out in the manifold harmonics domain by decomposing the embedding coordinates of the shape in this basis. However, since the basis functions depend on the shape itself, such filtering is valid only for weak (near all-pass) filters, and produces severe artifacts otherwise. In this paper, we analyze this problem and propose the fractional filtering approach, wherein we apply iteratively weak fractional powers of the filter, followed by the update of the basis functions. Experimental results show that such a process produces more plausible and meaningful results.

Keywords: Computational Geometry and Object Modeling, Hierarchy and geometric transformations, Laplace-Beltrami operator, 3D Mesh filtering.

1 Introduction

Different operations on the 3D data, such as noise removal, enhancement of specific parts of the object, may be formulated as applying filter $\mathbf{F}$ to the shape. It is well-known that the eigenfunctions of the Laplace-Beltrami operator (manifold harmonics) of a 3D shape (modelled as a 2-manifold) play the role of the Fourier basis in the Euclidean space [14,6]. Methods based on the Laplace-Beltrami operator have been used in a wide range of applications, among them remeshing [5,9], parametrization [2], compression [3], recognition [11,12], clustering, etc. Many methods in computer graphics and geometry processing draw inspiration from the world of physics, finding analogies between physical processes such as heat diffusion or wave equations [1] and the geometric properties of the shape [13]. Several works have studied consistent discretizations of the Laplace-Beltrami operator for the physical problems where this operator is involved [10,8,15]

Original shape   Standard filter   Fractional filter
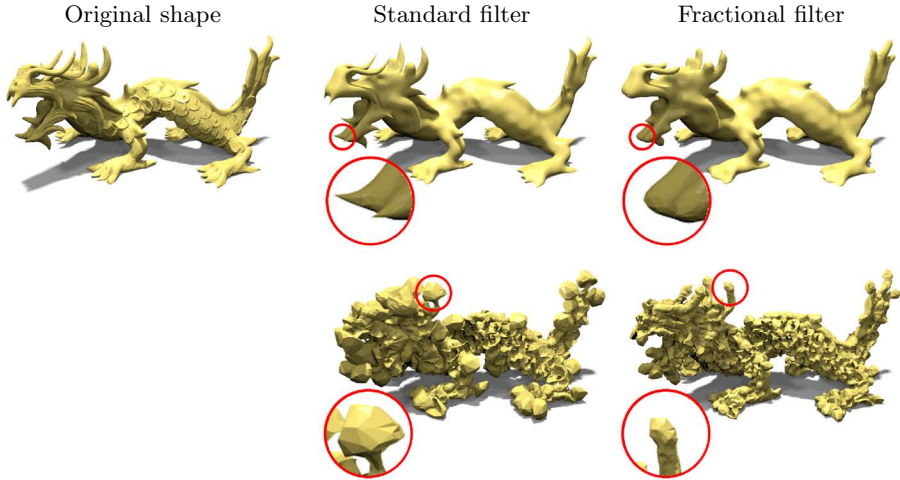
Fig. 1. Low- and band-pass filtering of the dragon shape (first column) using the Laplace-Beltrami filter (second column) and the proposed fractional approach (third column)

The influential paper of Taubin [14] drew the analogy between the classical signal processing theory and the manifold harmonics, showing that standard tools in signal processing such as analysis and synthesis of signals can be carried out on manifolds. This idea was extended in [4] and later in [7], showing a practical framework for shape filtering using the manifold harmonics transform.

One of the problematic issues in this approach is that, unlike the Euclidean case, where the basis functions are fixed, the manifold harmonics depend on the shape itself. Thus, filtering the shape changes the basis in which the filter coefficients are expressed. For strong filter, this may result in severe artifacts and unnatural behaviour.

Main Contribution. In this paper, we analyze this problem and propose the fractional filtering approach, wherein we apply iteratively weak fractional powers of the filter, followed by the update of the basis functions. The rest of the paper is organized as follows. We first review some notions in differential geometry and harmonic analysis in Section 2. In Section 3, we describe the filtering proposed in [7] and our fractional filtering approach. In Section 4 we show experimental results. Finally, Section 5 concludes the paper.

2   Background

In this section we briefly review the concept of manifold harmonics, and how to use it for approximating the shape filtering. For more detailed introduction reader referred to [14,7].

2.1 Manifold Harmonics

We model a shape as a compact two-dimensional manifold X, possibly with a boundary ∂X. Given a smooth scalar field f on the manifold X, the negative divergence of the gradient of a scalar field f, $\Delta f = -\operatorname{div} \operatorname{grad} f$, is called the *Laplacian* of f. For a general manifold the operator Δ is called the *Laplace-Beltrami* operator, and it generalizes the standard notion of the Laplace operator to manifolds. Note that we define the Laplacian with the negative sign to conform to the computer graphics and computational geometry convention.

Being a positive self-adjoint operator, the Laplacian admits an eigendecomposition

$$\Delta \phi = \lambda \phi \tag{1}$$

with non-negative eigenvalues λ and corresponding orthonormal eigenfunctions ϕ, where orthonormality is understood in the sense of the local inner product induced by the metric on the manifold. Furthermore, due to the assumption that our domain is compact, the spectrum is discrete, $0 = \lambda_1 < \lambda_2 < \cdots$.

In physics, (1) is known as the *Helmholtz equation* representing the spatial component of the wave equation. Thinking of our domain as of a vibrating membrane (with appropriate boundary conditions), the ϕ_i's can be interpreted as natural vibration modes of the membrane, while the λ_i's assume the meaning of the corresponding vibration frequencies. In fact, in this setting the eigenvalues have inverse area or squared spatial frequency units. We will denote the corresponding spatial frequencies as $\omega_i = \sqrt{\lambda_i}$ and use the two interchangeably. The eigenbasis of the Laplace-Beltrami operator is frequently referred to as the *harmonic basis* of the manifold, and the functions ϕ_i as *manifold harmonics*.

Given a square integrable function f on the manifold, satisfying certain boundary conditions when appropriate[1], it is well-established that f can be expanded into a Fourier series

$$f(x) = \sum_{i \geq 1} \hat{f}_i \phi_i(x) \tag{2}$$

with the coefficients

$$\hat{f}_i = \langle f, \phi_i \rangle = \int_X f(x) \phi_i(x) da(x). \tag{3}$$

The process of obtaining the coefficients $\hat{f}_i$ from f is usually referred to as *analysis*; the corresponding linear transformation will be dubbed as the *manifold harmonic transform* (MHT) after [7]. The inverse process obtained via the inverse MHT (IMHT) is known as *synthesis*.

---

[1] If the manifold has a boundary, ∂X, it is typical to enforce Dirichlet boundary conditions of the form $f|_{\partial X} = f_0$, or Neumann boundary conditions of the form $\langle \operatorname{grad} f, n \rangle|_{\partial X} = g_0$, where n denotes the normal to the boundary. Corresponding boundary conditions have to be imposed on the Laplace-Beltrami operator.

2.2   Discrete Manifold Harmonics

In the discretized setting, we represent the manifold X as a triangular mesh built upon the vertex set $\{\mathbf{x}_1, \ldots, \mathbf{x}_n\}$. A function f on the manifold is represented by the vector $\mathbf{f} = (f(\mathbf{x}_1), \ldots, f(\mathbf{x}_n))^{\mathrm{T}}$ of its samples. A common approach to discretizing manifold harmonics is by first constructing a discrete Laplace-Beltrami operator on the mesh, represented as a $n \times n$ matrix, followed by its eigendecomposition.

In our experiments we adopt a standard cotangent scheme [8]. The eigendecomposition results in the following generalized eigenvalue problem:

$$\mathbf{W}\phi_k = \mathbf{D}\lambda_k\phi_k \qquad (4)$$

where matrix $\mathbf{D}$ is diagonal, s.t. $D_{ii} = \frac{S_i}{3}$ (S_i - denotes area of all triangles sharing the vertex i), and $\mathbf{W}_{ij} = (\cot(\alpha_{ij}) + \cot(\beta_{ij}))/2, \mathbf{W}_{ii} = -\sum_j \mathbf{W}_{ij}$ (α_{ij}, β_{ij} are the two angles opposite to the edge between vertices i and j in the two triangles sharing the edge). In this case the the resulting eigenfunctions $\mathbf{\Phi}$ are $\mathbf{D}-$orthogonal [4], and the discrete MHT is expressed as multiplication by an $n \times n$ matrix $\mathbf{\Phi}^{\mathrm{T}}\mathbf{D}$, and IMHT is a multiplication by $\mathbf{\Phi}$. In the following we shortly will write $\mathbf{\Phi}^{\mathrm{T}}$ instead of $\mathbf{\Phi}^{\mathrm{T}}\mathbf{D}$, assuming that the appropriate inner product is considered.

3   Shape Filtering

In [7], Vallet and Lévy argued that the *extrinsic geometry* of a shape (i.e., the coordinates of the embedding of the manifold) can be thought of as a vector field $\mathbf{x} : X \to \mathbb{R}^3$ on the manifold and, hence, decomposed into

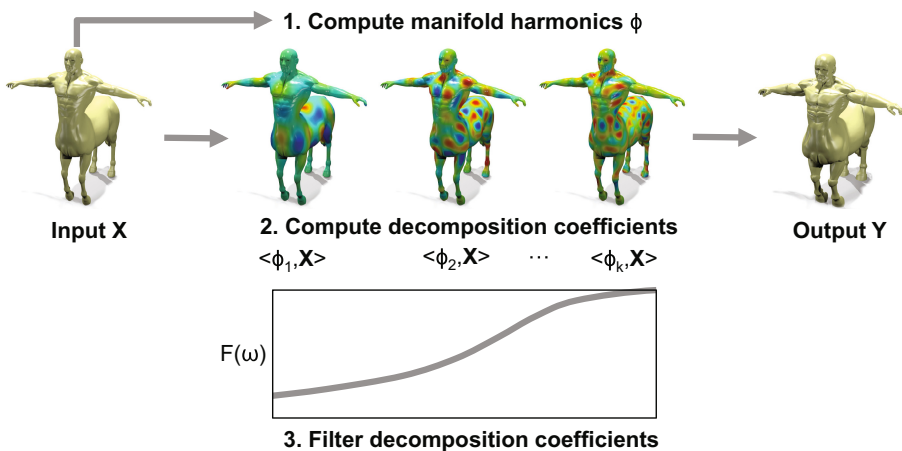**Fig. 2.** Pipeline of the Vallet-Lévy method

$$\mathbf{x} = \sum_{i \geq 1} \hat{\mathbf{x}}_i \phi_i \tag{5}$$

using the MHT, with $\hat{\mathbf{x}}_i = (\langle x^1, \phi_i \rangle, \langle x^2, \phi_i \rangle, \langle x^3, \phi_i \rangle)$, x^j denoting the j-th component of the vector $\mathbf{x}$. Since each Fourier coefficient is associated with a spatial frequency, the first coefficients can be interpreted as extrinsic geometric approximation of the shape, while the next ones correspond to the geometric details.

Analogously to the Fourier transform, the MHT separates frequencies, making the application of a filter $F(\omega)$ a simple product,

$$\mathbf{y} = \sum_{i \geq 1} F(\omega_i) \hat{\mathbf{x}}_i \phi_i. \tag{6}$$

The resulting embedding coordinates, $\mathbf{y} : X \rightarrow \mathbb{R}^3$, describe a new shape with frequency components changed according to the filter "transmission function" $F(\omega)$.

In practice, the above summation is truncated at some $i = k$ corresponding to ω_i, which is roughly comparable to the sampling radius of the shape. For that reason, fine geometric details do not participate in the analysis and synthesis, creating essentially a low-pass filter on top of $F(\omega)$. To counter this effect, Vallet and Lévy [7] proposed to compute the residual

$$\mathbf{e} = \sum_{i > k} F(\omega_i) \hat{\mathbf{x}}_i \phi_i = \mathbf{x} - \sum_{i=1}^{k} F(\omega_i) \hat{\mathbf{x}}_i \phi_i, \tag{7}$$

and re-inject it into the filtered shape by

$$\mathbf{y} = \sum_{i=1}^{k} F(\omega_i) \hat{\mathbf{x}}_i \phi_i + F_{\mathrm{h}} \mathbf{e}, \tag{8}$$

where F_{h} is the average filter response at $\omega \geq \omega_k$. In this way, the high frequency components are treated as a wave packet and filtered as a whole.

In the discrete setting, we represent the embedding of the shape as the $n \times 3$ matrix $\mathbf{X}$, and the response of the filter by the $k \times k$ diagonal matrix $\mathbf{F}(\boldsymbol{\omega_X}) = \mathrm{diag}\{F(\omega_1), \ldots, F(\omega_k)\}$. The discretized filter is given by

$$\mathbf{E} = (\mathbf{I} - \boldsymbol{\Phi_X} \boldsymbol{\Phi_X}^{\mathrm{T}}) \mathbf{X}$$
$$\mathbf{Y} = \boldsymbol{\Phi_X} \mathbf{F}(\boldsymbol{\omega_X}) \boldsymbol{\Phi_X}^{\mathrm{T}} \mathbf{X} + F_{\mathrm{h}} \mathbf{E}, \tag{9}$$

or alternatively by

$$\mathbf{Y} = (\boldsymbol{\Phi_X} \mathbf{F}(\boldsymbol{\omega_X}) \boldsymbol{\Phi_X}^{\mathrm{T}} + F_{\mathrm{h}} \bar{\mathbf{I}}_{\mathrm{h}}^{\mathbf{X}}) \mathbf{X}, \tag{10}$$

where $\boldsymbol{\Phi_X}$ is the $n \times k$ matrix representing the first k frequencies of the MHT and $\bar{\mathbf{I}}_{\mathrm{h}}^{\mathbf{X}} = \mathbf{I} - \boldsymbol{\Phi_X} \boldsymbol{\Phi_X}^{\mathrm{T}}$.

3. Update manifold harmonics ϕ

Input X

1. Compute decomposition coefficients

$\langle\phi_1,\mathbf{X}\rangle$ $\quad\quad\quad\langle\phi_2,\mathbf{X}\rangle$ $\quad\cdots\quad$ $\langle\phi_k,\mathbf{X}\rangle$

$F^{1/K}(\omega)$

2. Filter decomposition coefficients

Output $\mathbf{Y}^k$
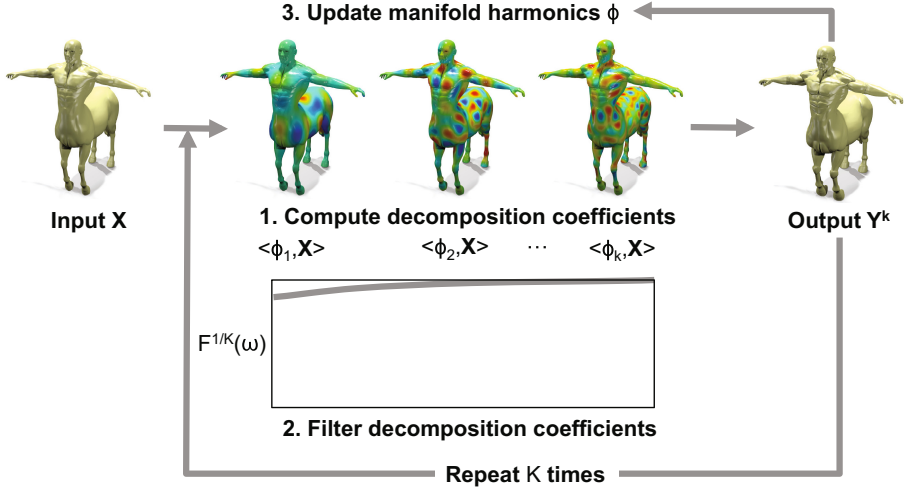
Repeat K **times**

Fig. 3. Pipeline of our method

3.1 Fractional Filter

It is important to note that the MHT $\boldsymbol{\Phi}_{\mathbf{X}}$ in (9) actually depends on $\mathbf{X}$ itself and *changes as a result of filtering.* However, Vallet and Lévy [7] do not account for this effect: their approach is correct only for infinitesimal change ($\mathbf{Y} \approx \mathbf{X}$), which is valid only if the filter is "weak" ($\mathbf{F} \approx \mathbf{I}$). For "strong" filters, such processing may result in severe artifacts (see Figure 1).

To counter this effect, we propose computing filters in an iterative manner, using fractional powers $\alpha < 1$ of the transfer function such that $F^\alpha \approx 1$. The fractional filter is computed according to (9) using $F^\alpha(\omega_i)$ as the transfer function; after each application, the Laplace-Beltrami operator and its eigenfunctions are recomputed. Setting $\alpha = 1/K$, the fractional filter is applied K times, resulting in the following intermediate results

$$\mathbf{Y}^{(k+1)} = (\boldsymbol{\Phi}_{\mathbf{Y}^{(k)}}\mathbf{F}^\alpha(\boldsymbol{\omega}_{\mathbf{Y}^{(k)}})\boldsymbol{\Phi}_{\mathbf{Y}^{(k)}}^{\mathrm{T}} + F_{\mathrm{h}}^\alpha\bar{\mathbf{I}}_{\mathrm{h}}^{\mathbf{Y}^{(k)}})\mathbf{Y}^{(k)}, \quad\quad (11)$$

The final result is

$$\mathbf{Y} = (\boldsymbol{\Phi}_{\mathbf{Y}^{(k-1)}}\mathbf{F}^\alpha(\boldsymbol{\omega}_{\mathbf{Y}^{(k-1)}})\boldsymbol{\Phi}_{\mathbf{Y}^{(k-1)}}^{\mathrm{T}} + F_{\mathrm{h}}^\alpha\bar{\mathbf{I}}_{\mathrm{h}}^{\mathbf{Y}^{(k-1)}})\cdots(\boldsymbol{\Phi}_{\mathbf{X}}\mathbf{F}^\alpha(\boldsymbol{\omega}_{\mathbf{X}})\boldsymbol{\Phi}_{\mathbf{X}}^{\mathrm{T}} + F_{\mathrm{h}}^\alpha\bar{\mathbf{I}}_{\mathrm{h}}^{\mathbf{X}})\mathbf{X}.$$

If all the eigenfunctions are used ($\boldsymbol{\Phi}$ is $n \times n$), the fractional filtering result is

$$\mathbf{Y} = \left(\boldsymbol{\Phi}_{\mathbf{Y}^{(K-1)}}\mathbf{F}^\alpha(\boldsymbol{\omega}_{\mathbf{Y}^{(K-1)}})\boldsymbol{\Phi}_{\mathbf{Y}^{(K-1)}}^{\mathrm{T}}\right)\cdots\left(\boldsymbol{\Phi}_{\mathbf{X}}\mathbf{F}^\alpha(\boldsymbol{\omega}_{\mathbf{X}})\boldsymbol{\Phi}_{\mathbf{X}}^{\mathrm{T}}\right)\mathbf{X},$$

as opposed to the standard approach where the eigenfunctions are not updated,

$$\mathbf{Y} = \left(\boldsymbol{\Phi}_{\mathbf{X}}\mathbf{F}^\alpha(\boldsymbol{\omega}_{\mathbf{X}})\boldsymbol{\Phi}_{\mathbf{X}}^{\mathrm{T}}\right)\cdots\left(\boldsymbol{\Phi}_{\mathbf{X}}\mathbf{F}^\alpha(\boldsymbol{\omega}_{\mathbf{X}})\boldsymbol{\Phi}_{\mathbf{X}}^{\mathrm{T}}\right)\mathbf{X}$$
$$= \boldsymbol{\Phi}_{\mathbf{X}}\mathbf{F}(\boldsymbol{\omega}_{\mathbf{X}})\boldsymbol{\Phi}_{\mathbf{X}}^{\mathrm{T}}.$$

Since the fractional filter is infinitesimal, the Laplacain does not change significantly between two applications of the filter; this allows to update efficiently the eigenfunctions $\boldsymbol{\Phi}$ as a perturbation of the Laplacian.
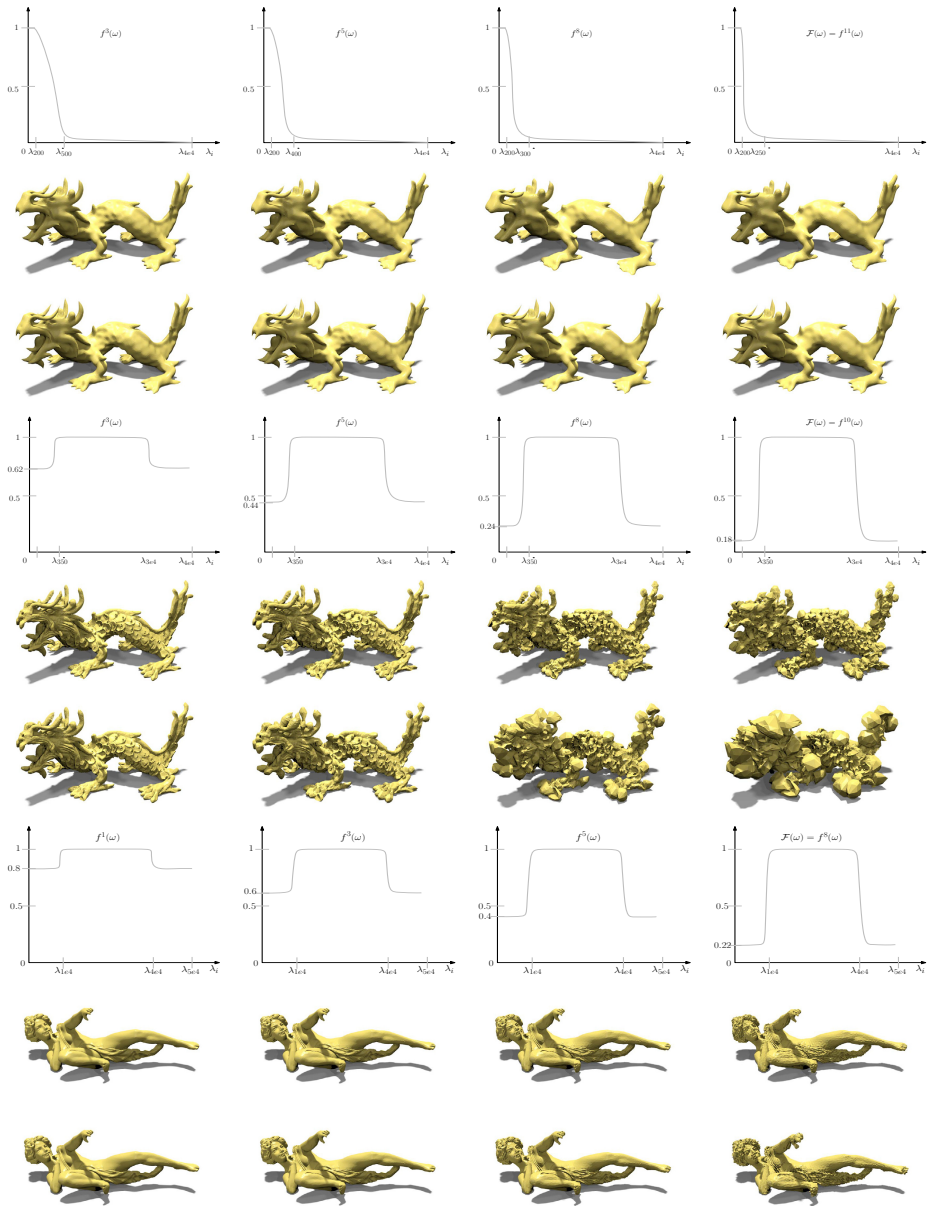
4   Results

In this section, we compare the standard filtering approach [7] with the proposed fractional filtering method. As test data, we used the *dragon* and *angel* shapes from the Stanford repository. The models were represented as triangular meshes with 4×10^4 and 5×10^4 vertices, respectively. Cotangent weight scheme was used to compute the discretization of the Laplace-Beltrami operator. In all the experiments, we used the full set of eigenvectors without resorting to the approximation proposed in [7] (treating high frequency components as a wave packet). We used two types of filters: low-pass and band-pass, with cutoff frequencies selected roughly according to the typical feature size on the shape. The fractional power was chosen in each case such that the resulting fractional filter is sufficiently weak.

Figure 5 shows the filtering results of the two shapes. We show the resulting shape after applying several times the fractional filter, without and with recomputation of the eigenbasis after each application. The final (rightmost) image is the filtering result. We can observe severe artifacts caused by the standard approach, such as sharp spikes on the dragon feet (unreasonable for a low-pass filter) and inflated ball-like structures on the dragon tail and angel fingers produced by the band-pass filter (see also Figure 1). Overall, our approach produces much more plausible and logical results: the low-pass filter result is smooth as expected, and the band-pass filter result has the effect of "feature enhancement" or sharpening.
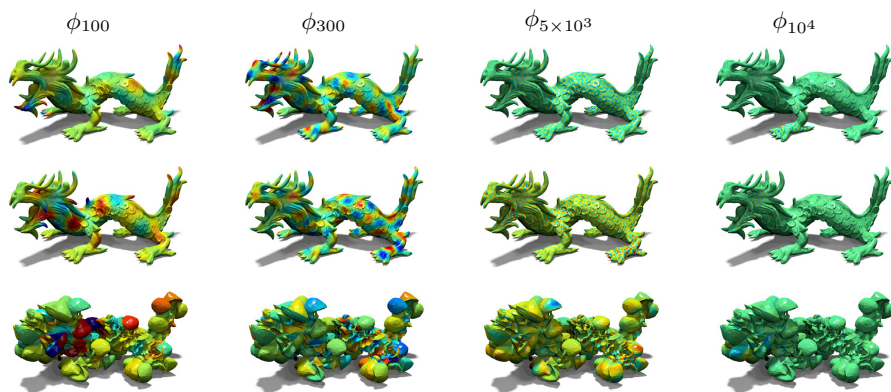
Fig. 4. The eigenfunctions of the Laplace-Beltrami operator of the dragon shape. Top: computed on original shape; middle: after 1/10 of a band-pass filter; bottom: after a full band-pass filter

Fig. 5. First, fourth and seventh rows: fractional powers of the filter; fractional filtering results with (second, fifth and eighth row) and without (third, sixth and ninth row) recompilation of the Laplacian basis

5   Conclusions

We analyzed the problem of shape filtering in the manifold harmonic transform domain and presented the fractional filtering method which allows to significantly reduce the artifacts observed when using strong filters. Our approach decomposes the filter into fractional powers and applies it sequentially, recomputing the Laplace-Beltrami eigenbasis after each application. Such a recomputation can be done efficiently as a small perturbation of the eigenvectors. Experimental results show that better results are obtained using this approach compared to direct filtering.

References

1. Coifman, R.R., Lafon, S.: Diffusion maps. Applied and Computational Harmonic Analysis 21, 5–30 (2006)
2. Floater, M., Hormann, K.: Surface parameterization: a tutorial and survey. Advances in Multiresolution for Geometric Modelling 1 (2005)
3. Karni, Z., Gotsman, C.: Spectral compression of mesh geometry. In: SIGGRAPH 2000: Proc. of the 27th Annual Conference on Computer Graphics and Interactive Techniques, pp. 279–286 (2000)
4. Kim, B., Rossignac, J.: Geofilter: Geometric selection of mesh filter parameters. Comput. Graph. Forum 24(3), 295–302 (2005)
5. Kobbelt, L.: Discrete fairing. In: Proc. of the Seventh IMA Conference on the Mathematics of Surfaces, pp. 101–131 (1997)
6. Lévy, B.: Laplace-Beltrami eigenfunctions towards an algorithm that "understands" geometry. In: Proc. SMA (2006)
7. Lévy, B., Zhang, R.H.: Spectral geometry processing. In: ACM SIGGRAPH ASIA Course Notes (2009)
8. Meyer, M., Desbrun, M., Schroder, P., Barr, A.H.: Discrete differential-geometry operators for triangulated 2-manifolds. In: Visualization and Mathematics III, pp. 35–57 (2003)
9. Nealen, A., Igarashi, T., Sorkine, O., Alexa, M.: Laplacian mesh optimization. In: Proc. of the 4th International Conference on Computer Graphics and Interactive Techniques in Australasia and Southeast Asia, pp. 381–389 (2006)
10. Pinkall, U., Polthier, K.: Computing discrete minimal surfaces and their conjugates. Experimental Mathematics 2(1), 15–36 (1993)
11. Reuter, M., Wolter, F.E., Peinecke, N.: Laplace-spectra as fingerprints for shape matching. In: Proc. ACM Symp. Solid and Physical Modeling, pp. 101–106 (2005)
12. Rustamov, R.M.: Laplace-beltrami eigenfunctions for deformation inavriant shape representation. In: Proc. of SGP, pp. 225–233 (2007)
13. Sun, J., Ovsjanikov, M., Guibas, L.J.: A concise and provably informative multi-scale signature based on heat diffusion. In: Proc. SGP (2009)
14. Taubin, G.: A signal processing approach to fair surface design. ACM (1995)
15. Wardetzky, M., Mathur, S., Kälberer, F., Grinspun, E.: Discrete Laplace operators: no free lunch. In: Conf. Computer Graphics and Interactive Techniques (2008)